

AN EQUIVALENT 4-WIRE LINE THEORETICAL MODEL OF REAL RFQ BASED ON THE SPECTRAL DIFFERENTIAL THEORY

F. Simoens, A. France, O. Delferriere, CEA-SACLAY, 91191 GIF/YVETTE

Abstract

A complete theoretical model has been developed within the context of RFQ tuning study. This model is based on an equivalent 4-wire line whose voltages obey a differential equation recast into an eigen-value problem. The segmentation and the non-homogeneity of the High Intensity Proton Injector (IPHI) RFQ are taken in account. Applying the spectral differential theory, the solutions of the eigen-value equation are the resonance modes. In this paper, the modes computed from our model are compared with experimental and 3D simulations results. The good agreement that we find validates our cut-off wave-guide equivalence approach.

1 RFQ 4-WIRE LINE MODEL

A new RFQ model [1] that we have developed is based on a 4-wire line supporting TEM modes that give a good image of the TE fields in the central region. Inverse inductances per unit length are added between each neighbouring lines in order to consider the longitudinal magnetic field H_z .

This model leads to a second order differential equation in voltage $\partial^2 \bar{U} / \partial z^2 - \bar{A} \bar{U} = -\omega^2 / c^2 \bar{U}$, where the matrix A contains all the electrical parameters of the line, and $\bar{U} = [U_Q, U_S, U_T]$ is the modal vector of the voltage, U_Q being the quadrupolar component, U_S and U_T the dipolar components.

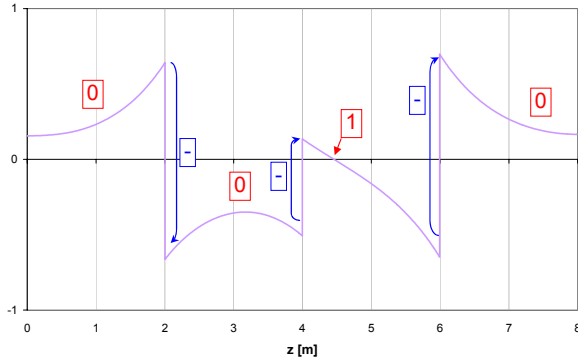


Fig. 1 : Example of a segmented "0-0-1-0" mode

The eigen-values of the equation are the frequencies of the resonance modes, the eigen-vectors correspond to the voltage profile between the electrodes. In a perfectly symmetrical RFQ, the Q, S and T eigen-spaces are decoupled and are described by 3 subsets of modal vectors vQ_i , vS_j and vT_k .

The figure 1 gives an example of the quadrupole resonance mode "0-0-1-0" computed in the case of the ideal IPHI RFQ (3 segments). The numbers stand for the number of times the voltage crosses zero within the

segment, the sign "--" signifies that a phase jump occurs in the corresponding coupling cell.

2 BEAD-PULL MEASUREMENTS ANALYSIS

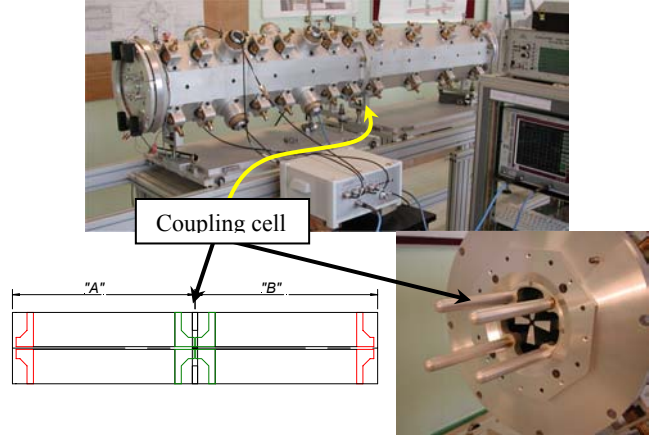


Fig. 2 : RFQ cold-model and the bead-pull test bench

Bead-pull measurements have been made in our RFQ cold-model configured as two coupled 1-m long segments (Fig. 2). The test bench [2] generates 4 vectors of perturbed phase $\varphi - \varphi_0$ (one per quadrant) as a function of the longitudinal position z , that can be written as :

$$\varphi - \varphi_0 = -\frac{d\varphi}{d\omega} \frac{\omega_0}{2} \left(f_{H//} \|\overline{H_{az}}\|^2 + f_{H\perp} \|\overline{H_{at}}\|^2 + f_{E\perp} \|\overline{E_{at}}\|^2 \right) \quad (1)$$

The subscript 'a' stands for normalization as defined by Slater [3], i.e. for example, the transverse component of the electric field E is $\overline{E_{at}} = \overline{E_t} / \sqrt{\int_{\Omega} \|\overline{E_{at}}\|^2 d\Omega}$.

The f parameters are the signed polarizabilities of the perturbing object with respect to its major ($//$) or minor (\perp) revolution axis. The equations of any TE mode [4] supported by the RFQ is given by :

$$\overline{E_t} = V(z) \vec{z} \times \nabla_t \psi(x,y), \quad \overline{H_t} = \frac{1}{j\omega\mu_0} \frac{dV(z)}{dz} \nabla_t \psi(x,y),$$

$$\overline{H_z} = \frac{1}{j\omega\mu_0} k^2 V(z) \psi(x,y) \vec{z}, \quad \text{where } V(z) \text{ is the voltage function, } \psi(x,y) \text{ is the modal function particular to the wave-guide mode present in each segment.}$$

The equation (1) takes the general form $\varphi - \varphi_0 = AV^2 + B(dV/dz)^2$, where $A > 0$ (resp. < 0) if the perturbing object is in a magnetically (resp. electrically) dominant region, and B is always > 0 . It follows that the wave-guide voltage is solution, up to an arbitrary multiplicative constant, of :

$$\pm (\varphi - \varphi_0) = y^2 + a(dy/dz)^2 \quad (2)$$

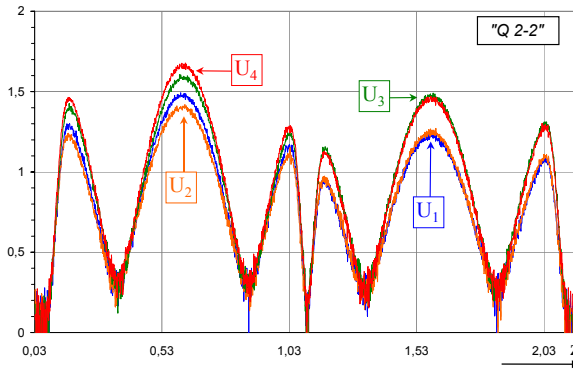


Fig. 3 : Line voltages of the quadrupole “2-2” mode (direct extraction as the square-root of $\varphi-\varphi_0$)

This equation explains why the direct extraction of the voltage as the square root of $\varphi-\varphi_0$ does not reach zero at the node positions of higher order modes (Fig. 3) .

mode	\tilde{a} [m ²]	$\pm 1 \sigma$
1-1	$1.04 \cdot 10^{-3}$	0.91 – 1.16
1+1	$9.75 \cdot 10^{-3}$	0.76 – 1.19
2-2	$1.12 \cdot 10^{-3}$	0.94 – 1.30
2+2	$1.13 \cdot 10^{-3}$	1.02 – 1.24
3-3	$1.31 \cdot 10^{-3}$	1.15 – 1.47
3+3	$1.26 \cdot 10^{-3}$	1.16 – 1.36

Table 1: Differential equation parameter a_{meas} .

First, the so-called ‘Differential Equation Parameter’ $a=B/A$, is directly estimated from the measurements at each node location; average values and standard deviations are given at the Table 1.

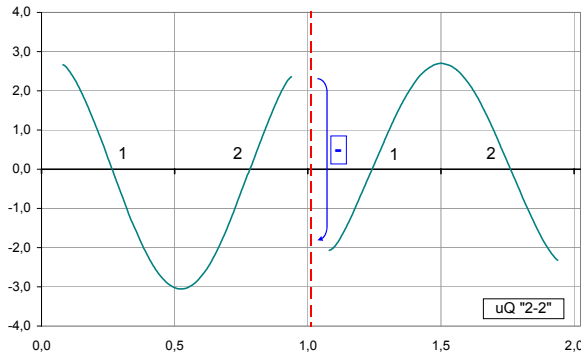


Fig. 4 : Line voltages of the quadrupole “2-2” mode

Once 'a' has been extracted, equation (2) is solved independently for each measured quadrant/segment of the RFQ, and ‘y’ is plotted vs. z (Fig. 4).

3 3D SIMULATIONS ANALYSIS

The 2-m long segmented RFQ has been meshed with IDEAS and the resonance modes have been found with the ‘Soprano’ RF modulus of Vector Fields (Fig. 5).

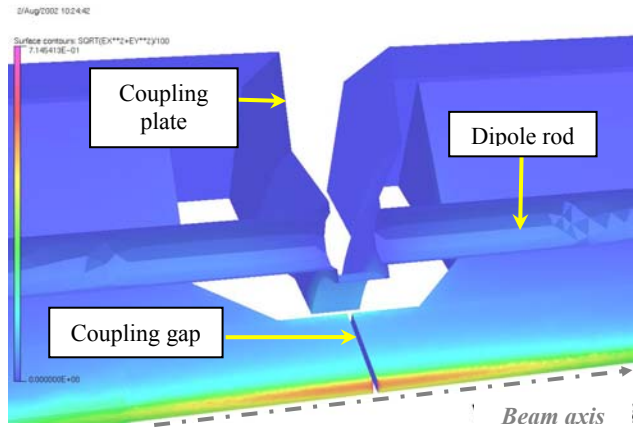


Fig. 5 : IPHI RFQ cold-model coupling cell

The simulation has generated the $|Et|$, H_z and $|Ht|$ (Fig. 6) as a function of z along the line on the bisector ($x = y = 55.15\text{mm}$) followed by the perturbing object.

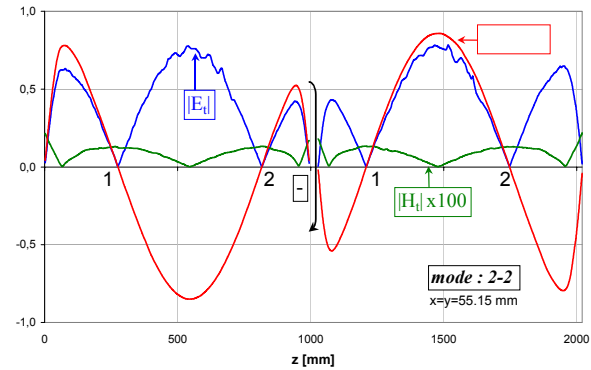


Fig. 6 : Field components computed by Soprano in the segment RFQ for the ‘2-2’ quadrupole mode

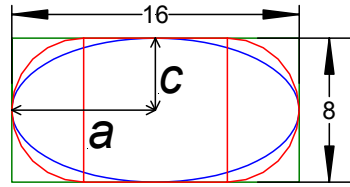


Fig. 7 : Perturbing object (red)

The perturbing object volume is bounded by a cylindrical volume and an ellipsoidal volume (Fig. 7).

The polarizability factors can be analytically computed for these 2 last geometries as :

	Ellipsoid ([5])	Cylinder ([6])
$f_{E\perp}$	$1,2975 \cdot 10^{-6}$	$1,8522 \cdot 10^{-6}$
$f_{H\parallel}$	$0,6288 \cdot 10^{-6}$	$0,9261 \cdot 10^{-6}$
$f_{H\perp}$	$0,9137 \cdot 10^{-6}$	$1,3155 \cdot 10^{-6}$

We can compute the differential equation parameter from the simulated fields components and the ‘f’ parameters as :

$$a_{th} = \frac{f_{H\perp} E_t^2}{\omega^2 \mu_0^2 [f_{H\parallel} H_z^2 - f_{E\perp} E_t^2 (1/\eta^2)]}$$

ω = resonance frequency, η = vacuum impedance.

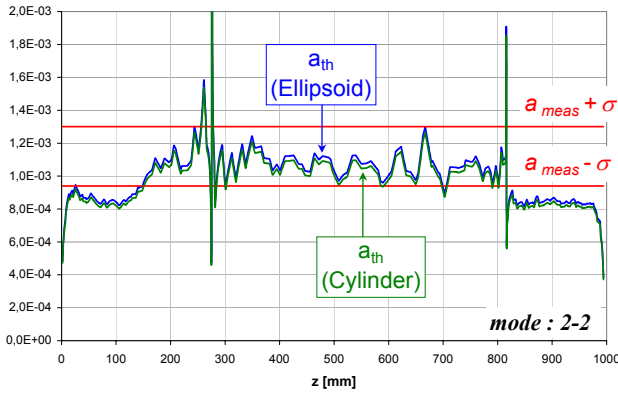


Fig. 8 : Differential Equation Parameter comparison

a_{th} as a function of z in the first section has been plotted. For the set of measured segmented modes (Table 1), a_{th} is perfectly bounded by $a_{meas.} \pm \sigma$ for either bead geometries, ellipsoid or cylinder (Fig. 8). Note that a perfectly sinusoidal voltage function would yield a constant a_{th} , and discrepancies observed in the end regions of the segment are mainly due to mesh inaccuracies.

4 COMPARISONS WITH OUR MODEL

At this point we can compare: (i) resonance frequencies f_Q and ' $y(z)$ ' functions extracted from measurements, (ii) f_Q , Et and/or H_z computed by the 3D simulation code, (iii) eigen-values f_{Qi} and eigen-vectors v_{Qi} numerically computed from the RFQ 4-wire line model (where the coupling capacitance has been set to 1,85 pF).

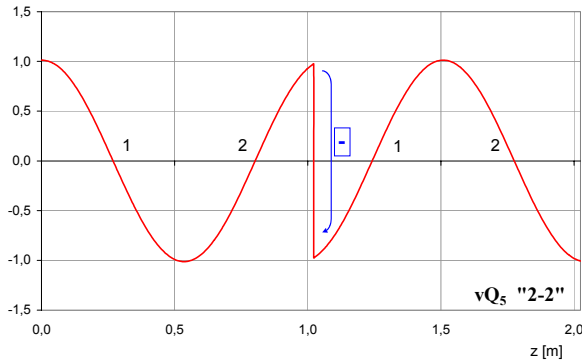


Fig. 9 : Eigen-vector of the quadrupole '2-2' mode

Sorted in ascending frequency order, these three sets of 'voltage' functions agree perfectly, with the same number of zeros in their respective segments, and nodes located at the same longitudinal positions (compare Fig. 4, 6 & 9). Measured and simulated frequencies are also in good accordance, up to an additive constant, mainly due to mesh limitations (Table 2 & Fig. 10). The eigen-values f_{Qi} of the 4-wire line model are close to the measured frequencies for low order modes. The segmented modes frequencies ('2-2', '3-3', ...) diverge as orders increase, because the frequency dispersivity of the coupling susceptance is not included in our model.

i	mode	$f_{Q_{meas}}$	$f_{Q_{Soprano}}$ simulations	$f_{Q_{4-wire}}$ line model
1	0-0	340,50	339,47	340,56
2	0+0	350,85	348,43	350,84
3	1-1	369,53	368,01	370,59
4	1+1	380,28	378,89	380,37
5	2-2	445,17	443,56	449,45
6	2+2	458,64	456,59	457,66
7	3-3	550,16	548,11	556,71
8	3+3	566,68	564,10	563,37

Table 2: Quadrupole resonance frequencies comparison

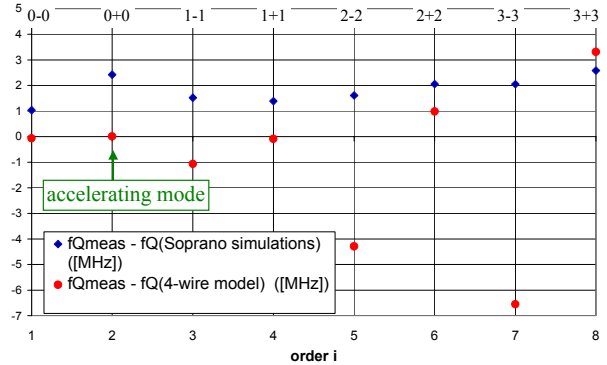


Fig. 10 : Frequency difference between measurements, simulations (Soprano) and our model.

5 CONCLUSION

The close agreement between measurements, 3D and 4-wire line simulations supports the analogy between RFQ's and TE-mode wave-guides, either for the accelerating mode or the other higher order modes: (i) voltage and voltage derivative profiles of a segmented RFQ are precisely reproduced, (ii) eigen-frequencies are predicted with an accuracy compatible with tuning requirements, (iii) effects of a perturbing bead are quantitatively predicted.

6 REFERENCES

- [1] A. France, F. Simoens, "Theoretical Analysis of a Real-life RFQ Using a 4-Wire Line Model and the Spectral Theory of Differential Operators", EPAC2002, Paris, 2002
- [2] F. Simoens & al., "A Fully Automated Test Bench for the Measurement of the Field Distribution in RFQ and Other Resonant Cavity", EPAC2002, Paris, 2002.
- [3] J.C. Slater, "Microwave Electronics", Van Nostrand Company Inc., 1959 fifth edition
- [4] R.N. Ghose, "Microwave Circuit Theory and Analysis", Mc Graw-Hill, 1963
- [5] L.C. Maier, JR. and J.C. Slater, "Field Strength Measurements in Resonant Cavities", MIT, Journal of Applied Physics, vol 23, Number 1, pp 68-77, 1952
- [6] K. M. Siegel, "Far field scattering from bodies of revolution", Appl. Sci. Res, Section B, Vol. 7, 1957